J Physiol 588.12 (2010) pp 2147–2162

The Journal of Physiology

Acid-sensing ion channels in rat hypothalamic vasopressin neurons of the supraoptic nucleus

Toyoaki Ohbuchi[1,2], Kaori Sato[3], Hideaki Suzuki[2], Yasunobu Okada[3], Govindan Dayanithi[4], David Murphy[5] and Yoichi Ueta[1]

Departments of [1] Physiology and [2] Otorhinolaryngology, School of Medicine, University of Occupational and Environmental Health, Kitakyushu, Japan
[3] Department of Cell Physiology, National Institute for Physiological Sciences, Okazaki, Japan
[4] Department of Cellular Neurophysiology, Institute of Experimental Medicine, Academy Sciences of the Czech Republic, European Union Research Center of Excellence, Prague, Czech Republic
[5] Laboratories of Integrative Neurosciences and Endocrinology, University of Bristol, Bristol, UK

Body fluid balance requires the release of arginine vasopressin (AVP) from the neurohypophysis. The hypothalamic supraoptic nucleus (SON) is a major site of AVP synthesis, and AVP release is controlled somatodendritically or at the level of nerve terminals by electrical activities of magnocellular neurosecretory cells (MNCs). Acid-sensing ion channels (ASICs) are neuronal voltage-insensitive cationic channels that are activated by extracellular acidification. Although ASICs are widely expressed in the central nervous system, functional ASICs have not been assessed in AVP neurons. ASICs are modulated by lactate (La^-), which reduces the extracellular calcium ion concentration. We hypothesize that ASICs modify neuronal function through La^- that is generated during local hypoxia resulting from osmotic stimulation in the SON. In the present study, we used the whole-cell patch-clamp technique to show that acid-induced ASIC current is enhanced by La^- in isolated rat SON MNCs that express an AVP-enhanced green fluorescent protein (eGFP) transgene. Immunohistochemistry and multi-cell reverse transcriptase-polymerase chain reaction experiments revealed that these neurons express the ASIC1a and ASIC2a subunits. In addition, increased La^- production was specifically observed in the SON after osmotic stress. These results suggest that interaction between ASICs and La^- in the SON plays an important role in the regulatory mechanism of body fluid homeostasis.

(Received 20 January 2010; accepted after revision 26 April 2010; first published online 4 May 2010)
Corresponding author Y. Ueta: 1-1 Iseigaoka, Yahatanishi-ku, Kitakyushu 807-8555, Japan.
Email: yoichi@med.uoeh-u.ac.jp

Abbreviations ASIC, acid-sensing ion channel; AVP, arginine vasopressin; GFP, green fluorescent protein; La^-, lactate; MNC, magnocellular neurosecretory cell; OXT, oxytocin; SON, supraoptic nucleus.

Introduction

The hypothalamic supraoptic nucleus (SON) is a major site of synthesis of arginine vasopressin (AVP) and oxytocin (OXT). Magnocellular neurosecretory cells (MNCs) in the SON project into the neurohypophysis and release AVP into the systemic circulation in response to various physiological and/or pathological stimuli including body fluid volume, osmolality (Leng *et al.* 1999; Sharif Naeini *et al.* 2006), acute systemic hypoxia (Smith *et al.* 1995), and nociception (Suzuki *et al.* 2009). The release of these hormones is closely related to the electrical activity of the MNCs, which in turn are regulated by neuronal synaptic inputs (Leng *et al.* 1999). Since synaptic vesicles have an intravesicular pH of 5.6, neurons are constantly exposed to local acidosis resulting from proton diffusion from presynaptic vesicles (Miesenbock *et al.* 1998). In addition, a recent study has shown that osmotic stimulation causes tissue hypoxia as a result of constriction of local arterioles via stimulation of perivascular V_{1a}-receptors by AVP that is locally released from dendrites in the rat SON (Alonso *et al.* 2008). Because hypoxia stimulates cellular lactate (La^-) production in the central nervous system (CNS) (Ronne-Engström *et al.* 1995; Vannucci *et al.* 1994), these reports led us to hypothesize that local acidosis and La^- modulation play important roles in regulating the activity of AVP neurons in the SON.

Acid-sensing ion channels (ASICs) are neuronal voltage-insensitive cation channels that are activated by extracellular acidification and potentiated by reduced extracellular Ca^{2+} concentration induced by La^-

DOI: 10.1113/jphysiol.2010.187625

(Waldmann *et al.* 1997; Immke & McCleskey, 2001). They belong to the epithelial amiloride-sensitive Na^+ channel and degenerin (ENaC/DEG) family of ion channels (Kellenberger & Schild, 2002) that share common structural features of two transmembrane domains, short intracellular N and C termini, and a large cysteine-rich extracellular loop. Four ASIC genes (ASIC1–4) encoding seven isoforms (ASIC1a and its splice variants ASIC1b and ASIC1b2, ASIC2 splice variants ASIC2a and ASIC2b, ASIC3, and ASIC4) have been described in mammals (Price *et al.* 1996; Waldmann *et al.* 1996; Garcia-Anoveros *et al.* 1997; Lingueglia *et al.* 1997; Chen *et al.* 1998; Akopian *et al.* 2000; Grunder *et al.* 2000). A recent crystal structure study suggests that ASICs are trimeric assemblies of ASIC subunits (Jasti *et al.* 2007). ASICs are widely expressed in the peripheral and central nervous system where they perform physiological functions. Several ASIC subunits are present in brain, including ASIC 1a, 2a, and 2b, with significant overlap of expression (Krishtal, 2003; Voilley, 2004; Wemmie *et al.* 2006; Lingueglia, 2007).

In the present study, we characterized the functional and biochemical properties of ASIC-mediated currents and potentials in isolated rat SON MNCs that express an AVP-enhanced green fluorescent protein (eGFP) transgene (Ueta *et al.* 2005) using a whole-cell patch-clamp technique. Multi-cell reverse transcriptase-polymerase chain reaction (RT-PCR) revealed expression of mRNA encoding ASICs 1a and 2a, but not the other subunits. Furthermore, ASIC-mediated responses of AVP neurons were enhanced by lowering extracellular Ca^{2+} or by addition of La^-.

We also demonstrated increased La^- production in the SON of rats after salt loading but not after euhydration. Together, La^--induced potentiation of ASIC activity in AVP neurons and the induction of La^- in the SON following osmotic stress suggest an involvement of ASICs and La^- modulation in the regulatory mechanisms of body fluid balance.

Methods

Animals

Experiments were performed on a total of 72 male Wistar rats or transgenic rats aged 3–5 weeks (young adult, weighing 80–150 g) that express an AVP-eGFP fusion gene (Ueta *et al.* 2005). Animals were housed in standard plastic cages at 23–25°C on a 12 h light (07.00–19.00 h)–12 h dark cycle. All experiments in this study were carried out in accordance with the guidelines of the Physiological Society of Japan under the control of the Ethics Committee of Animal Care and Experimentation, University of Occupational and Environmental Health, Japan. Our experiments comply with *The Journal of Physiology*'s policies and regulations (Drummond, 2009).

Solutions

The solution used in the experiments with SON slice preparations was a modified Krebs–Henseleit solution (KHB) containing 124 mM NaCl, 5 mM KCl, 1.3 mM $MgSO_4$, 1.24 mM KH_2PO_4, 2 mM $CaCl_2$, 25.9 mM $NaHCO_3$ and 10 mM glucose. The solution was continuously oxygenated with a mixture of 95% O_2–5% CO_2. The solution used in the experiments with dissociated neurons was a Hepes buffered solution (HBS) containing 140 mM NaCl, 5 mM KCl, 1.2 mM KH_2PO_4, 2 mM $CaCl_2$, 1.2 mM $MgCl_2$, 10 mM glucose and 10 mM Hepes, adjusted to pH 7.4 with NaOH. This solution was continuously oxygenated with 100% O_2.

In Na^+-free medium, Na^+ was replaced with equimolar *N*-methyl-D-glucamine (NMDG) (Sigma), and in Ca^{2+}-free medium, Ca^{2+} was replaced with 5 mM EGTA. For the measurement of Na^+ permeability, the external solution contained 140 mM NaCl, 10 mM Hepes, and 10 mM glucose. For experiments examining the effect of lactate, the control bath solution contained 110 mM NaCl, 5 mM KCl, 1.2 mM KH_2PO_4, 2 mM $CaCl_2$, 1.2 mM $MgCl_2$, 10 mM glucose, and 10 mM Hepes. Lactate solutions were prepared by adding sodium lactate (Sigma) to this solution and adjusting the final Na^+ concentration to 140 mM with sodium gluconate. Other monocarboxylic acid solutions were prepared by substituting sodium lactate with sodium pyruvate, sodium formate, sodium butyrate, or sodium acetate (all from Sigma). Acidic solutions were buffered using a combination of 10 mM Hepes and 10 mM 2-(*N*-morpholino)ethanesulfonic acid (Mes) (Sigma). The osmolarity of the isotonic solution and hypertonic solution was 300 mosmol l^{-1} and 350 mosmol l^{-1}, respectively. The osmolarity of the hypertonic solution and culture medium was adjusted with mannitol. The pipette solution used in the recording electrodes contained 140 mM potassium gluconate, 1 mM $MgCl_2$, 1 mM $CaCl_2$, 10 mM EGTA, 10 mM Hepes, and 2 mM Mg-ATP, adjusted to pH 7.3 with Tris base. For measurement of Na^+ permeability, 140 mM sodium gluconate was used instead of 140 mM potassium gluconate.

Supraoptic nucleus slice preparation

Young adult male Wistar rats or AVP-eGFP transgenic rats were killed by decapitation. The brains were quickly removed, taking care to avoid gross contusion or haemorrhage during and after removal of the brain from the skull, and cooled in KHB at 4°C for 1 min. A block containing the hypothalamus was cut from the brain and glued onto the stage of a vibrating blade tissue slicer (Linearslicer Pro 7, DSK, Kyoto, Japan). After careful removal of the meninges, 500 μm coronal slices containing the SON were cut from the block in KHB at 4°C as previously described (Kabashima *et al.* 1997). The slices

were carefully trimmed with a circular punch (inner diameter 1.8 mm) and pre-incubated in KHB at room temperature (22–24°C) for 1 h before enzyme digestion or culture.

Dissociation of AVP-eGFP transgenic rat SON neurons and cell culture

SON neurons of AVP-eGFP rats were dissociated by an enzymatic digestion method (Ohbuchi *et al.* 2009). Briefly, SON slices were incubated in 4 ml HBS containing DNase I (Sigma, 0.5 mg ml^{-1}) and papain (20 U ml^{-1}; Worthington Biochemical Corp., Lakewood, NJ, USA) in a 50 ml Eppendorf tube with 100% oxygen for 50 min at 30°C. The slices were then transferred to normal HBS and washed for at least 1 h prior to mechanical dissociation by trituration with fire-polished glass pipettes. The cell suspension was plated onto coverslips placed individually in wells of multiwell culture plates with 2 ml culture medium and maintained in a humidified incubator at 37°C with 5% CO_2 for 1 day. The culture medium was Neurobasal-A medium (Invitrogen) supplemented with 0.5 mM L-glutamine, B27 (Invitrogen), 5 ng ml^{-1} fibroblast growth factor (Sigma), and penicillin–streptomycin (Invitrogen). The osmolarity of the culture medium was adjusted to 300 ± 5 mosmol l^{-1} with NaCl.

Single-cell patch-clamp

The coverslip with plated neurons was placed in a glass-bottomed chamber and continuously perfused with HBS at a rate of 1.5 ml min^{-1} using an eight-head peristaltic pump (MP-8, Gilson nucleus, Villiers le Bel, France). The volume of the recording chamber was 1 ml. The solution level was kept constant by a low-pressure aspiration system. Isolated MNCs expressing AVP-eGFP were identified by their green fluorescence. The electrodes used in this study were triple-pulled from a glass capillary with a puller (P-87, Sutter Instrument Co., Novoto, CA, USA). The pipettes had a final resistance of 5–8 MΩ when filled. An axopatch 200B amplifier (Axon Instruments) was used to record ionic currents in the tight-seal, whole-cell configuration. Acidic solutions and all drugs were pressure-applied via a Y-tube system (Xu *et al.* 1999), a rapid drug exchange technique that allows the external solution surrounding a neuron to be exchanged within 20 ms. The Y-tube tip was positioned 1.5 mm from the recording electrode in the cell body. Membrane voltages and currents were controlled and recorded with a computer running pCLAMP8 software (Molecular Devices, Sunnyvale, CA, USA). To calculate the reversal potential, the liquid junction potential correction for 24°C was made with pCLAMP8 software. In the present case, the corrected potential value was the measured potential minus 13.1 mV in the whole-cell recording configuration. Recording commenced at least 3 min after membrane rupture when the currents reached a steady state. Recordings included in data analysis were collected during periods of stable series resistance. All experiments were carried out at room temperature (22–24°C).

Multi-cell RT-PCR

The coverslip containing the plated neurons was placed in a glass-bottomed chamber with 2 ml sterilized HBS. Isolated MNCs expressing AVP-eGFP were identified by their green fluorescence. Positive pressure was applied to the pipette (inner tip diameter, 10–20 μm), and the pipette was then targeted to AVP-eGFP neurons. After the pipette was attached to a cell, the positive pressure was removed and negative pressure applied to harvest cytoplasmic contents. Cytoplasmic contents of five AVP-eGFP neurons were harvested under visual control and pooled in a PCR tube with carrier RNA (poly-A RNA, Qiagen, Valencia, CA, USA). Total RNA was purified using an RNeasy Micro Kit (Qiagen), and heated with 5 μM Oligo dT primer (Takara Bio Inc., Shiga, Japan) and 1 mM dNTP mixture (Takara) at 65°C for 5 min then cooled on ice. The reverse transcription mixture (40 μl) contained these pooled cytoplasmic samples, 1× PrimeScript Buffer (Takara), 40 U RNase inhibitor (Takara), and 200 U PrimeScript RTase (Takara). Reverse transcription was carried out at 42°C for 60 min. After stopping the reaction at 70°C for 15 min, products were stored at −20°C until use. We performed PCR amplification of mRNA transcripts of AVP and ASIC subunits in a 50 μl reaction containing 3.3 μl of the reverse transcription mixture as template, 1× Ex Taq Buffer, 0.2 mM dNTP mixture, 0.12 μM forward and reverse primers, and 0.05 U Ex Taq (Takara) with the following amplification conditions: 94°C for 30 s; 40 cycles of 94°C for 30 s, 55°C for 1 min, 72°C for 1 min; and 72°C for 5 min. The amplified products were separated by electrophoresis on 2% agarose gels, stained with ethidium bromide, and visualized under UV irradiation. Gel images were captured using AE-6905H Image Saver HR (Atto, Tokyo, Japan). For ASICs, the following sets of primers were used: 5′-CACAGATGGCTGATGAAAAGCAG-3′ (forward)/5′-CATGGTAACAGCATTGCAGGTGC-3′ (reverse) for ASIC1a (Nagae *et al.* 2007) (GenBank accession no. NM_024154, product size 506 bp); 5′-ATGCCGTGCGGTTGTCCC-3′ (forward)/5′-CATGGTAACAGCATTGCAGGTGC-3′ (reverse) for ASIC1b (Nagae *et al.* 2007) (GenBank accession no. AJ309926, product size 563 bp); 5′-ATCTCTGCCTTGAATGCCAAGGTT-3′ (forward)/5′-AACTCCCCAGCGTGGTACAAGT-3′ (reverse) for ASIC2a (GenBank accession no. NM_001034014, product size 443 bp); 5′-CTGCCTTCATGGACCGTTTG-3′ (forward)/5′-CGAGTCCCATCTCTGAGGACCGG-3′ (reverse) for ASIC2b

(Kawamata *et al.* 2006) (GenBank accession no. NM_012892, product size 429 bp); 5′-GATCCAGAGCCCTCTGATCCCTTGGG-3′ (forward)/5′-ATTCAACTCTTCCTGGAGCAGA-3′ (reverse) for ASIC3 (GenBank accession no. NM_173135, product size 603 bp); 5′-TCTGCCCGCCAAATATCTAC-3′ (forward)/5′-ATGCTAGCCCCAATGAACAG-3′ (reverse) for ASIC4 (Brockway *et al.* 2005) (GenBank accession no. NM_022234, product size 334 bp). As a positive control, we amplified glyceraldehyde-3-phosphate-dehydrogenase (GAPDH) using the following primers: 5′-CATGCCGCCTGGAGAAACCTGCCA-3′ (forward)/5′-GGGCTCCCCAGGCCCCTCCTGT-3′ (reverse) (GenBank accession no. NM_017008.3, product size 429 bp). These primer sets were selected from previous reports (Brockway *et al.* 2005; Kawamata *et al.* 2006; Nagae *et al.* 2007) or were newly designed using Primer3 software (http://frodo.wi.mit.edu/) with confirmation of their specificity to the complementary sequences in the rat genome by NCBI BLAST (http://www.ncbi.nlm.nih.gov/blast/). We also performed the whole procedure without addition of reverse transcriptase (RT–) and obtained negative results. To confirm the specific expression of mRNA in AVP-eGFP neurons, we performed RT-PCR for GFP transcripts on five AVP-eGFP positive cells and five AVP-eGFP negative cells using the following primers: 5′-CACCATCTTCTTCAAGGACGAC-3′ (forward)/ 5′-ATGATATAGACGTTGTGGCTGTTGT-3′ (reverse) (GenBank accession no. YP002302326.1, product size 186 bp) (Ueta *et al.* 2005). We observed a band corresponding to GFP in all samples ($n = 6$) from five AVP-eGFP-positive cells, whereas no bands corresponding to GFP were detected in any of the samples ($n = 3$) from five AVP-eGFP-negative cells (data not shown).

Immunohistochemistry

Isolated cells were fixed overnight with phosphate-buffered saline (PBS) containing 4% paraformaldehyde and washed with PBS at room temperature. After 1 h incubation with 1% fetal bovine serum (FBS) and 0.3% Triton X-100, cells were washed and incubated overnight at 4°C with ASIC1 polyclonal antibody (1:4000) (Donier *et al.* 2005; Foulkes *et al.* 2006; Vila-Carriles *et al.* 2006; Vukicevic *et al.* 2006; Meltzer *et al.* 2007), ASIC2a polyclonal antibody (1:4000) (Alvarez de la Rosa *et al.* 2002), or ASIC3 polyclonal antibody (1:2000) (all from Alomone Labs, Jerusalem, Israel) (Ye *et al.* 2007). After washing, cells were incubated for 1 h with fluorescently labelled secondary antibody Alexa Fluor 546 goat anti-rabbit IgG (1:1000; Invitrogen). Images were acquired using a fluorescence microscope.

Measurements of SON La^- and pyruvate

To assess the effect of osmotic stimulation on La^- release, SON slices were incubated in multiwell culture plates containing 1 ml normal culture medium or hypertonic culture medium in a humidified incubator at 37°C with 95% air and 5% CO_2 for 24 h. To evaluate the effect of hypoxia on La^- release, SON slices were incubated in multiwell culture plates containing 1 ml normal culture medium in a humidified incubator at 37°C with a mixture of 85% N_2–10% O_2–5% CO_2 for 24 h. The culture medium was collected and deproteinized by $HClO_4$ for determination of the amount of La^- and pyruvate released from SON. La^- and pyruvate concentrations were measured by enzyme assays using lactate oxidase and pyruvate oxidase, respectively.

For *in vivo* experiments, adult male Wistar rats were euhydrated or salt-loaded by drinking 2% NaCl for 5 days, then killed by decapitation. SON slices were prepared as described above. Bilateral SON segments were quickly frozen in liquid nitrogen and powdered frozen tissue was deproteinized using $HClO_4$. La^- and pyruvate concentrations were measured by enzyme assays using lactate oxidase and pyruvate oxidase, respectively.

Data analysis

All data are normalized to basal level. Results were expressed as the mean ± S.E.M. Statistical comparisons were performed with Student's *t* test or Welch's *t* test. Analysis of variance (ANOVA) for multiple comparisons was used as noted in Fig. 1*H*. In all cases, $P < 0.05$ (*) or 0.01 (**) was considered significant.

Results

Identification of ASIC currents in cultured AVP-eGFP neurons

Primary cell cultures derived from the SON of AVP-eGFP transgenic rats were established as described previously (Ueta *et al.* 2005; Ohbuchi *et al.* 2009). To determine whether AVP neurons can be activated by lowering extracellular pH, we performed whole-cell voltage-clamp recordings in cultured AVP-eGFP SON neurons identified by their green fluorescence.

When the neurons were held at −70 mV, fast reduction of the extracellular pH evoked rapidly desensitizing inward currents with an average decay time constant of 1.94 ± 0.07 s ($n = 57$). The peak amplitude of these acid-induced currents showed high sensitivity to pH, with an activation threshold of ∼pH 6.8. Between pH 7.4 and 4.0, activation of the peak current could be fitted by a sigmoidal curve, with a half-maximum activation pH value (pH_{50}) of 5.71 ± 0.04 and Hill slope factor of

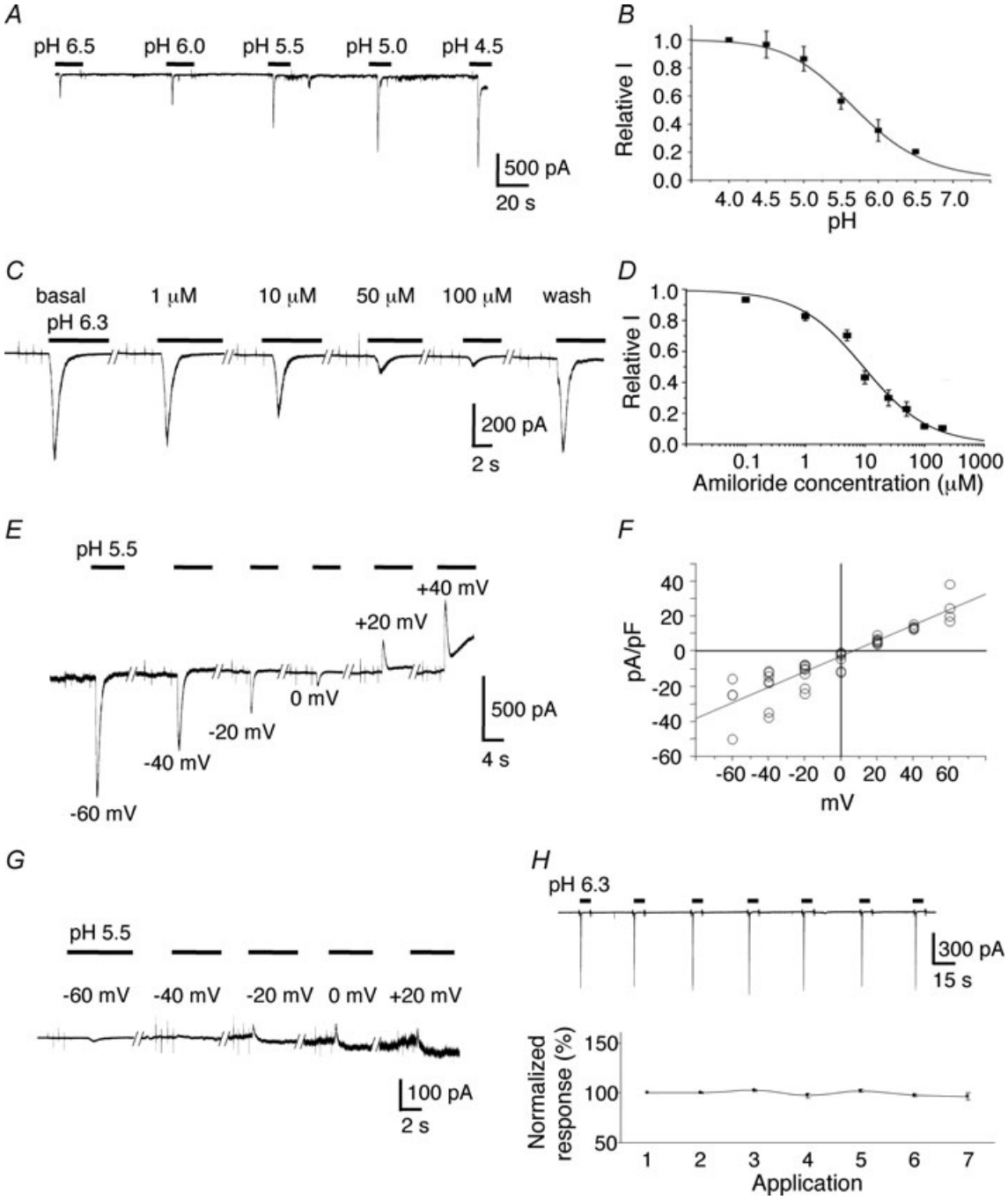

Figure 1. Acid-induced currents in AVP-eGFP neurons
A, typical traces showing currents induced by extracellular solutions with different pH. *B*, all values were normalized to the peak amplitude of a pH 4.0-induced current. Data were fitted to a sigmoidal curve with a pH_{50} value of 5.71 ± 0.04 ($n = 3$–9). *C*, representative example of the effect of amiloride, a classic blocker of ASICs. *D*, all values were normalized to the peak amplitude of a pH 6.3-induced current. Data were fitted to a sigmoidal curve with an IC_{50} value of 9.51 ± 1.2 μM ($n = 4$–7). *E*, typical recordings of pH 5.5-induced currents at different holding potentials. *F*, *I–V* curve of pH 5.5-induced current showing that the reversal potential was +7.2 mV when equimolar Na^+ (140 mM) was present in both intracellular and extracellular solutions ($n = 3$–8). *G*, typical recordings of pH 5.5-induced currents at different holding potentials when the extracellular Na^+ was replaced by NMDG. *H*, application of a pH 6.3 solution for 5 s at 30 s intervals to the same cells seven times did not significantly reduce current amplitude. The data were analysed using one-way ANOVA followed by a Tukey–Kramer type adjustment for multiple comparisons.

0.99 ($n = 3$–9; Fig. 1*A* and *B*). The peak current could be reversibly inhibited in a concentration-dependent manner by amiloride (Sigma), a known selective blocker of cloned ASICs (Waldmann *et al.* 1997), with a half-maximal inhibition (IC_{50}) value of $9.51 \pm 1.2\ \mu$M and Hill slope factor of 0.98 ($n = 4$–7; Fig. 1*C* and *D*). The acid-induced current was not inhibited by $10\ \mu$M ruthenium red ($94.8 \pm 2.7\%$ of basal, $P > 0.05$, $n = 5$; Fig. 2*A*,*E*), ruling out contamination by acid-activated TRPV1 and TRPA1 currents. We then analysed the Na^+ permeability of the acid-activated channels. pH 5.5-induced currents were recorded in AVP-eGFP neurons at different holding potentials from −60 mV to +60 mV. When equimolar Na^+ (140 mM) was present in both extracellular and intracellular solutions, the measured reversal potential of acid-induced currents was +7.2 mV ($n = 3$–8; Fig. 1*E* and *F*). The reversal potential value after correction for junction potential was −5.9 mV, which is close to the theoretical Na^+ equilibrium potential (0 mV). When the extracellular Na^+ was replaced with NMDG, the amplitude of the acid-induced current was markedly reduced or virtually eliminated ($n = 4$; Fig. 1*G*), indicating that the acid-induced current in AVP-eGFP neurons is primarily carried by Na^+, and that other cations appear to play a minor role. Repetitive addition of pH 6.3 solution to the same cells seven times for 5 s at 30 s intervals did not significantly decrease the current amplitude, which varied between 96.5 and 102.4% of the first application ($P > 0.05$, $n = 4$; Fig. 1*H*), indicating that the 30 s interval of acid application is sufficiently long for ASICs to fully recover from desensitization.

The presence of $300\ \mu$M Zn^{2+}, which is known to increase the amplitude of ASIC currents flowing through ASIC2a-containing channels (Baron *et al.* 2001), increased the peak ASIC current in AVP neurons ($173 \pm 15\%$ of basal, $P < 0.01$, $n = 7$; Fig. 2*B* and *E*). The ASIC currents in AVP neurons induced at pH 6.3 were not inhibited by 100 nM Psalmotoxin (PcTX1, Peptide Institute, Inc., Osaka, Japan), a peptide derived from the venom of a Trinidad chevron tarantula and a specific blocker of homomeric ASIC1a channels (Escoubas *et al.* 2000, 2003; Bubien *et al.* 2004; Chen *et al.* 2005, 2006; Salinas *et al.* 2006; Qadri *et al.* 2009) ($87.9 \pm 7.5\%$ of basal, $P > 0.05$, $n = 5$; Fig. 2*C* and *E*). Similarly, $1\ \mu$M PcTX1 did not decrease the amplitude of the ASIC current ($93.5 \pm 7.9\%$ of basal, $P > 0.05$, $n = 3$; data not shown). The absence of functional ASIC3 was indicated by the insensitivity of ASIC currents to 1 mM salicylate (Sigma), an ASIC3 subunit blocker (Voilley *et al.* 2001) ($91.5 \pm 7.0\%$ of basal, $P > 0.05$, $n = 4$; Fig. 2*D* and *E*). In 5 out of 104 neurons tested at pH 6.3 in the normal external solution, a sustained component that did not inactivate while the pH remained acidic was recorded in addition to the transient current (Fig. 2*F*). Because this represented a minor fraction of the neurons, data were not used in analyses if a sustained plateau phase following the peak current was observed. Current-clamp recordings showed that the activation of ASICs by pH 6.8 induced depolarization, which accompanied the appearance of a single action potential (Fig. 2*G*). The transient depolarization induced by lowering the pH from 7.4 to 6.3 could trigger a train of action potentials. In all six neurons examined, the depolarization was highly attenuated by the ASIC inhibitor amiloride ($100\ \mu$M). Similarly, blocking the voltage-gated Na^+ channel with $1\ \mu$M tetrodotoxin (Alomone labs) completely eliminated the action potentials induced by the low pH solution in all six neurons.

ASICs 1 and 2a are expressed in isolated eGFP-AVP neurons in rat SON

We immunostained isolated MNCs of SONs that expressed the AVP-eGFP transgene with antibodies against ASIC1, 2a and 3. MNCs expressing AVP-eGFP showed positive staining for ASIC1 and −2a, but not for ASIC3 (Fig. 3*A*), indicating that AVP neurons in the SON express ASIC1 and ASIC2a proteins.

Transcription of ASICs in AVP neurons

To investigate expression of ASIC mRNAs in AVP neurons, we performed RT-PCR using cytoplasmic samples collected from multiple AVP neurons under the whole-cell configuration. Template cDNA was subjected to RT-PCR with specific primers for ASIC 1a, 1b, 2a, 2b, 3, and 4 subunits, and GAPDH. Positive bands were observed for ASIC 1a and 2a subunits, but not for 1b, 2b, 3, and 4 subunits (Fig. 3*B*). The GAPDH reaction was positive in all samples. Bands corresponding to the 1a and 2a subunits and GAPDH were sequenced and confirmed to be identical to known mRNA sequences of rat ASICs and GAPDH, respectively.

La^- enhances acid-induced currents in AVP-eGFP neurons

Lactate does not directly activate ASICs. Currents induced by a change to pH 6.3 increased in the presence of lactate at a concentration of 3 mM ($0.69 \pm 1.0\%$ increase from basal, $P > 0.05$ compared with basal, $n = 5$), 7.5 mM ($4.18 \pm 2.3\%$ increase from basal, $P > 0.05$ compared with basal, $n = 5$), 15 mM ($18.4 \pm 2.8\%$ increase from basal, $P < 0.01$ compared with basal, $n = 19$), and 30 mM ($31.1 \pm 9.8\%$ increase from basal, $P < 0.01$ compared with basal, $n = 5$) (Fig. 4*A*). The proton dose response of the currents in the presence or absence of lactate showed that the lactate effect was lost at lower pH (Fig. 4*B*). Lactate (15 mM) potentiated the acid-induced current at pH 5.5 ($2.03 \pm 1.7\%$ increase from basal, $P > 0.05$ compared

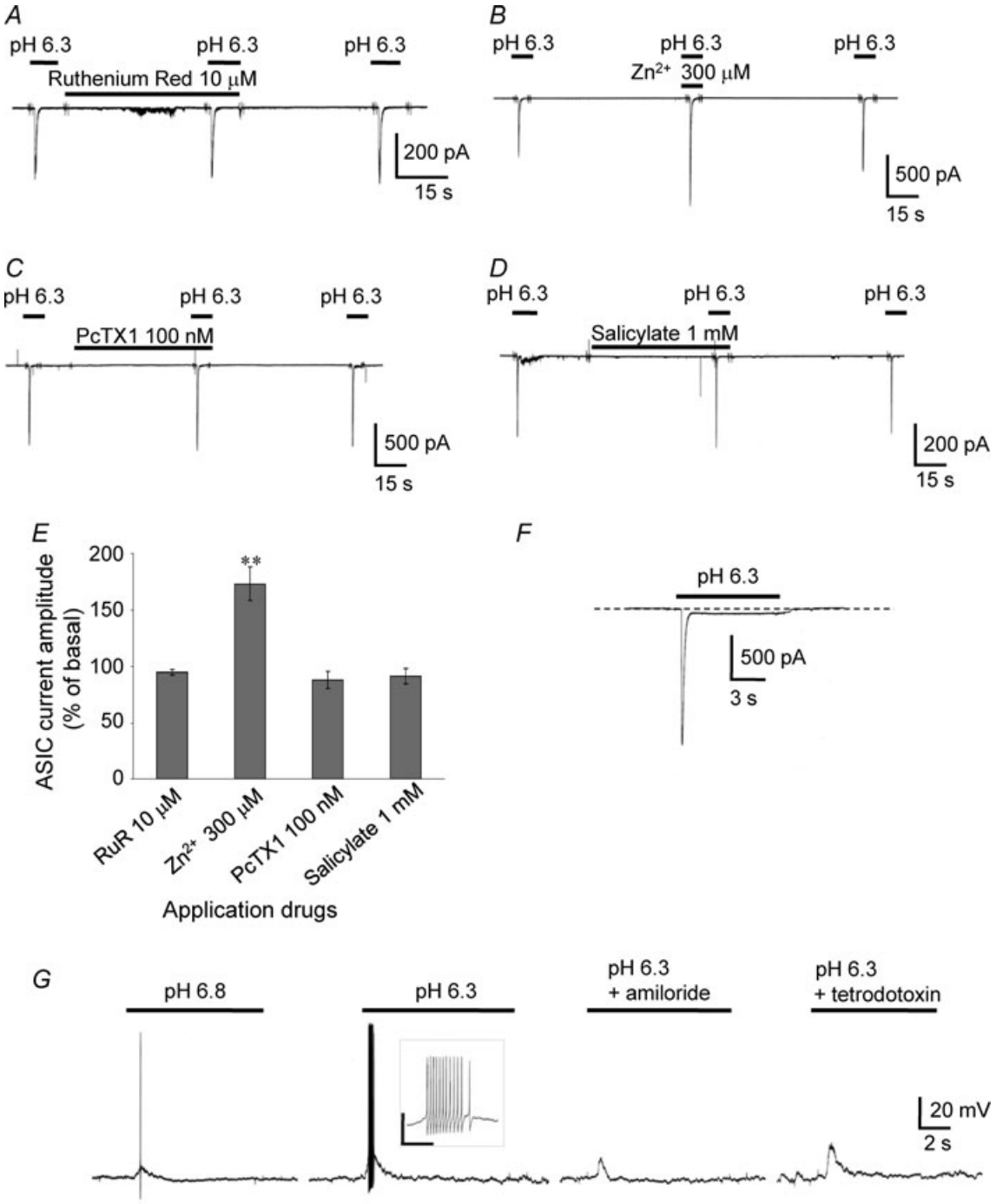

Figure 2. Properties of acid-induced responses in AVP-eGFP neurons
A, representative example of the effects of 10 μM ruthenium red (RuR), a TRPV1 and TRPA1 antagonist. *B*, representative example of the effects of 300 μM Zn^{2+}, a co-activator of ASIC2a-containing channels. *C*, representative example of the effects of 100 nM PcTX1, a specific blocker of homomeric ASIC1a. *D*, representative example of the effects of 1 mM salicylate, an ASIC3 subunit blocker. *E*, comparison of the effects of ruthenium red, Zn^{2+}, PcTX1, and salicylate on peak amplitude of pH 6.3-induced currents. The holding potential was −70 mV. Vertical bars indicate S.E.M.; $^{**}P < 0.01$ compared with basal. *F*, representative trace of the sustained plateau phase following the peak current. *G*, activation of ASICs by pH 6.8-induced depolarization accompanied by the appearance of a single action potential. The transient depolarization induced by lowering the pH from 7.4 to 6.3 could trigger a train of action potentials (inset). The depolarization was highly attenuated by the ASIC inhibitor 100 μM amiloride ($n = 6$). Blocking voltage-gated Na^+ channels with 1 μM tetrodotoxin completely eliminated the action potentials induced by the low pH solution ($n = 6$). Inset: the scale bar is 50 mV/0.3 s.

with basal, $n = 4$), pH 6.3 ($18.4 \pm 2.8\%$ increase from basal, $P < 0.01$ compared with basal, $n = 19$), and pH 6.8 ($47.5 \pm 7.5\%$ increase from basal, $P < 0.01$ compared with basal, $n = 11$). Currents induced at the peak amplitude of pH 6.8 were used only if a change evoked >100 pA. Lactate enhanced the current only if it was applied with the stimulating solution and a 30 s preincubation with lactate had no effect on the subsequent acid-induced current, suggesting that lactate does not act through an intracellular signalling cascade (Fig. 4*C*).

Previous studies have indicated that lactate acts through its ability to chelate extracellular calcium ions (Immke & McCleskey, 2001). The pH 6.3 gated current was potentiated by 0 mM Ca^{2+} ($135 \pm 8.8\%$ of 2 mM Ca^{2+}, $P < 0.01$, $n = 16$) and 1 mM Ca^{2+} ($125 \pm 11\%$ of 2 mM Ca^{2+}, $P < 0.05$, $n = 6$), but inhibited by 5 mM Ca^{2+} ($62.9 \pm 7.4\%$ of 2 mM Ca^{2+}, $P < 0.05$, $n = 4$) and 10 mM Ca^{2+} ($41.5 \pm 6.4\%$ of 2 mM Ca^{2+}, $P < 0.01$, $n = 4$). Thus, the pH 6.3-induced current was potentiated by low extracellular Ca^{2+} concentration, and the current enhancement induced by lactate was eliminated under this condition, indicating that the effects of lactate are due to calcium chelation (Fig. 5*A* and *D*). In contrast, the pH 6.3 gated current was inhibited by higher extracellular Ca^{2+} concentrations (Fig. 5*B* and *C*). A calcium dose–response of the currents in the presence or absence of lactate showed that the lactate effect is greater at higher calcium concentrations and showed saturation up to 5 mM (Fig. 5*C* and *D*). Fifteen millimolar lactate enhanced the pH 6.3-induced currents at calcium concentrations of 0 mM ($0.38 \pm 0.8\%$ increase from basal, $P > 0.05$ compared with basal, $n = 6$), 2 mM ($18.4 \pm 2.8\%$ increase from basal, $P < 0.01$ compared with basal, $n = 19$), 5 mM ($51.8 \pm 13\%$ increase from basal, $P < 0.05$ compared with basal, $n = 4$), and 10 mM ($53.1 \pm 18\%$ increase from basal, $P < 0.05$ compared with basal, $n = 4$).

Lactate, pyruvate and formate each enhanced the ASIC current, whereas acetate and butyrate had no

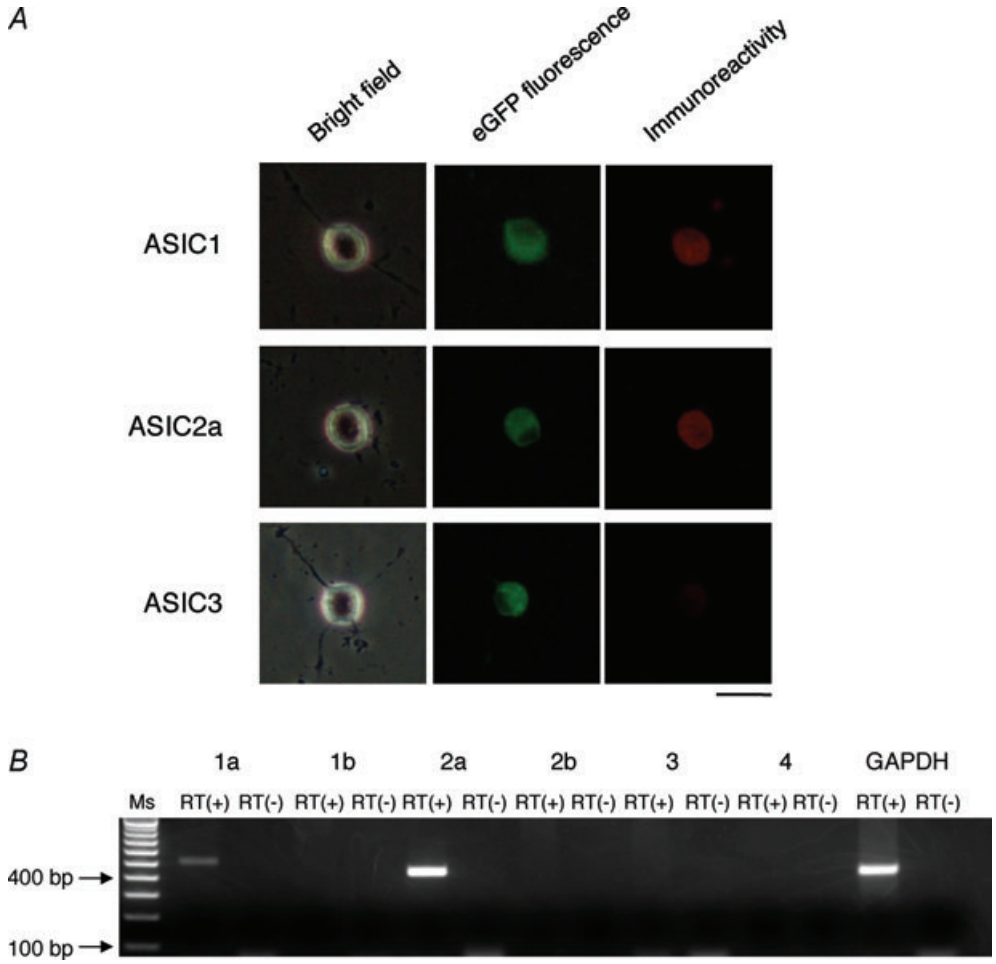

Figure 3. Expression of ASIC subunits in AVP-eGFP neurons in the SON
A, immunostaining showed expression of ASIC1 and ASIC2a, but not ASIC3. Red indicates immunostaining for ASIC subunits, green indicates expression of AVP-eGFP. Scale bar indicates 50 μm. *B*, multi-cell RT-PCR revealed expression of mRNA encoding ASICs1a and -2a but not mRNA encoding the other subunits. Ms indicates 100-bp marker ladder, RT(–) indicates negative control lacking reverse transcriptase.

effect. Figure 5*E* shows the effect of 15 mM lactate (18.4 ± 2.8% increase from basal, $P < 0.01$ compared with basal, $n = 19$), 15 mM pyruvate (5.74 ± 3.6% increase from basal, $P < 0.05$ compared with basal, $n = 8$), 15 mM formate (4.3 ± 2.6% increase from basal, $P < 0.05$ compared with basal, $n = 8$), 15 mM butyrate (0.42 ± 4.0% increase from basal, $P > 0.05$ compared with basal, $n = 5$), and 15 mM acetate (–2.91 ± 1.6% increase of basal, $P > 0.05$ compared with basal, $n = 5$) on the pH 6.3-induced current. Hyperosmolality had no effect on the acid-induced current amplitude, lactate enhancement, or desensitization (Fig. 5*F*).

Effect of La^- on the acid-induced excitability of AVP-eGFP neurons

We also examined variation in membrane potential when acidic stimulation was applied to AVP neurons

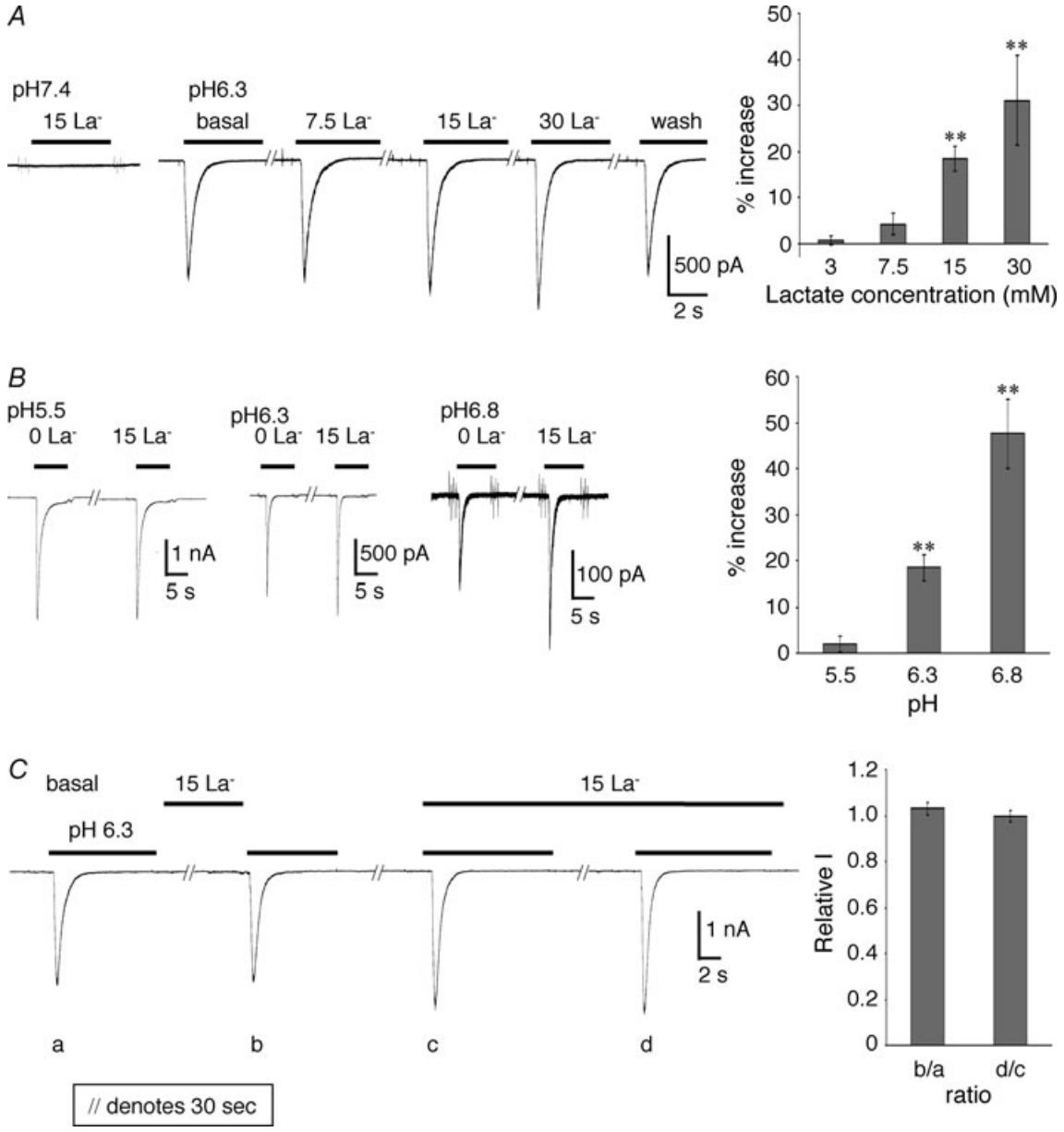

Figure 4. Effects of lactate on acid-induced currents in AVP-eGFP neurons
A, lactate enhances acid-gated currents in a concentration-dependent manner and does not directly activate ASICs. Currents induced by a change to pH 6.3 increased with lactate concentration and showed no saturation up to 30 mM. *B*, proton dose response of the currents in the presence or absence of 15 mM lactate. *C*, lactate enhanced the current only if it was applied with the stimulating solution and 30 s preincubation had no additional effect. The ratio of 'b' to 'a' is 1.03 ± 0.03, and that of 'd' to 'c' is 0.99 ± 0.03 ($P > 0.05$ compared with each basal, $n = 4$).

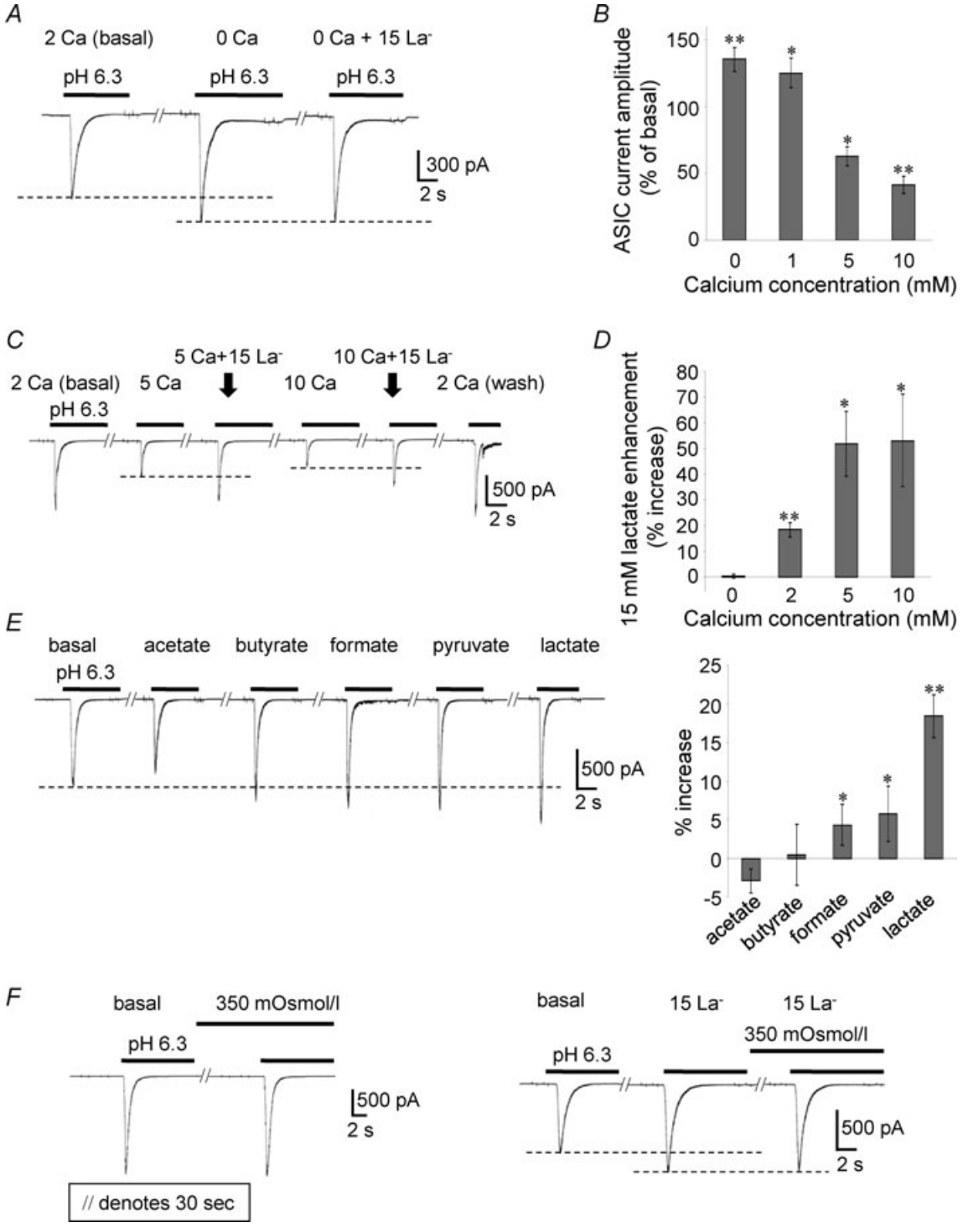

Figure 5. Effects of lactate through chelation of extracellular calcium
A and *B*, the pH 6.3 gated current was potentiated by 0 mM Ca^{2+} and 1 mM Ca^{2+}, and inhibited by 5 mM Ca^{2+} and 10 mM Ca^{2+}. *C* and *D*, the calcium dose response of the pH6.3-induced currents in the presence or absence of 15 mM lactate shows that the lactate effect is greater at higher calcium concentrations. *E*, the effect of 15 mM lactate, 15 mM pyruvate, 15 mM formate, 15 mM butyrate, and 15 mM acetate on the pH 6.3-induced current. *F*, hyperosmolality had no effect on the pH 6.3-induced current amplitude or lactate enhancement ($P > 0.05$ compared with each basal, $n = 3$).

under the current clamp condition. Typical changes in membrane potential elicited by decreasing the pH from 7.4 to 6.8 in the presence or absence of lactate are shown in Fig. 6*A*. Activation of ASIC current by pH 6.8 transiently depolarized the neurons. When a pH 6.8 external solution containing 15 mM lactate was applied, the neuron was depolarized with a train of action potentials at the initial transient depolarization (Fig. 6*A* inset). When cells were held at a level around the firing threshold with a current injection, pH 6.8-induced depolarization and action potentials were observed, followed by a refractory period (Fig. 6*B*). Lactate increased the depolarization and firing number induced by pH 6.8 (Fig. 6*B* inset). These results indicate that the lactate-modulated activation of ASICs regulates the excitability of AVP neurons.

Osmotic stimulation induces La^- release in the SON

We next measured the amount of La^- and pyruvate released from the SON under normal and hypertonic conditions. Isolated SON tissues were incubated in a culture medium at 300 mosmol l^{-1} or 350 mosmol l^{-1} at 37°C for 24 h then La^- and pyruvate concentrations in the medium were measured by enzyme assays using lactate oxidase and pyruvate oxidase, respectively. The SON segment incubated under hypertonic conditions showed greater La^- secretion than the segment in isotonic conditions ($108 \pm 2.7\%$ of control, $P < 0.05$, $n = 12$) (Fig. 6*C*); however, there was no difference in the amount of pyruvate released into the medium under the two conditions ($104 \pm 1.5\%$ of control, $P > 0.05$, $n = 12$) (Fig. 6*C*). The tissue La^- level in the SON was significantly increased after osmotic stimulation resulting from salt loading by drinking 2% NaCl for 5 days ($122 \pm 7.5\%$ of control, $P < 0.05$, $n = 9$), whereas the tissue pyruvate level in the SON was markedly decreased after osmotic stimulation ($69.1 \pm 0.1\%$ of control, $P < 0.01$, $n = 5$). Moreover, the tissue La^-:pyruvate ratio was increased in the SON of salt-loaded rats ($154 \pm 6.3\%$ of control, $P < 0.01$, $n = 5$) (Fig. 6*D*).

Hypoxic stimulation induces La^- release in the SON

We further measured the amount of La^- and pyruvate released from SON into the extracellular medium under normoxic or hypoxic conditions. Isolated SON tissues were incubated in a normal culture medium at 37°C with 95% air–5% CO_2 or a mixture of 85% N_2–10% O_2–5% CO_2 for 24 h, then La^- and pyruvate concentrations in the medium were measured. The SON segment incubated under hypoxic conditions with 85% N_2–10% O_2–5% CO_2 showed higher La^- secretion ($114 \pm 3.9\%$ of control, $P < 0.05$, $n = 5$) and lower pyruvate secretion ($76.7 \pm 2.0\%$ of control, $P < 0.01$, $n = 5$) than the segment in normoxic conditions with 95% air–5% CO_2. The La^-:pyruvate ratio in the medium released from SON was significantly increased under hypoxia ($148 \pm 3.8\%$ of control, $P < 0.01$, $n = 5$). As a result, hypoxia significantly increased the La^-:pyruvate ratio in the medium surrounding the SON (Fig. 6*E*).

Discussion

ASICs play important roles in physiological and pathological conditions of the nervous system, particularly in the CNS, and have been reported to be involved in synaptic plasticity (Wemmie *et al.* 2002), pain sensation (Duan *et al.* 2007), and ischaemia (Xiong *et al.* 2004; Gao *et al.* 2005). ASICs are activated by extracellular acidification; the contents of synaptic vesicles are acidic (pH 5.6), and a transient drop in extracellular pH is associated with synaptic transmission (Miesenbock *et al.* 1998).

The SON consists of two types of MNC that synthesize AVP or OXT, and identification of cell type is particularly important in the isolated single-cell patch-clamp studies since AVP and OXT neurons display considerably different electrophysiological properties (Hirasawa *et al.* 2003; Leng *et al.* 1999; Li *et al.* 2007). In the present study, AVP neurons were identified using transgenic rats that express an eGFP fusion gene in AVP-containing MNCs. Our results demonstrate that heteromeric ASIC1a+ASIC2a channels are responsible for proton-induced currents in the majority of SON AVP neurons. We also show that La^- potentiates the activity of ASICs in AVP neurons. The increase in lactate production in the SON following osmotic stimulation suggests involvement of ASICs and their modulation by La^- in central osmotic sensing under pathological conditions.

Identification of ASICs in the SON AVP neurons

In the present study, we demonstrate that extracellular acidification induced an amiloride-sensitive ($IC_{50} = 9.51\ \mu M$) transient inward current characterized by rapid desensitization with an average decay time constant of 1.94 ± 0.07 s, an activation threshold of ~pH 6.8, pH_{50} of 5.71, and Hill slope factor of 0.99. These results indicate that acid-induced currents in rat SON AVP neurons are mediated by functional ASICs. Our results provide evidence that the ASICs in these neurons are heteromeric ASIC1a+ASIC2a channels through the observations that ASIC-like currents were not altered by PcTX1 but were enhanced by Zn^{2+}, and that the acid sensitivity of the AVP neurons, the average decay time constant, activation threshold, and pH_{50} value are similar to those observed for ASC1a+ASIC2a heteromeric channels expressed in *Xenopus* oocytes

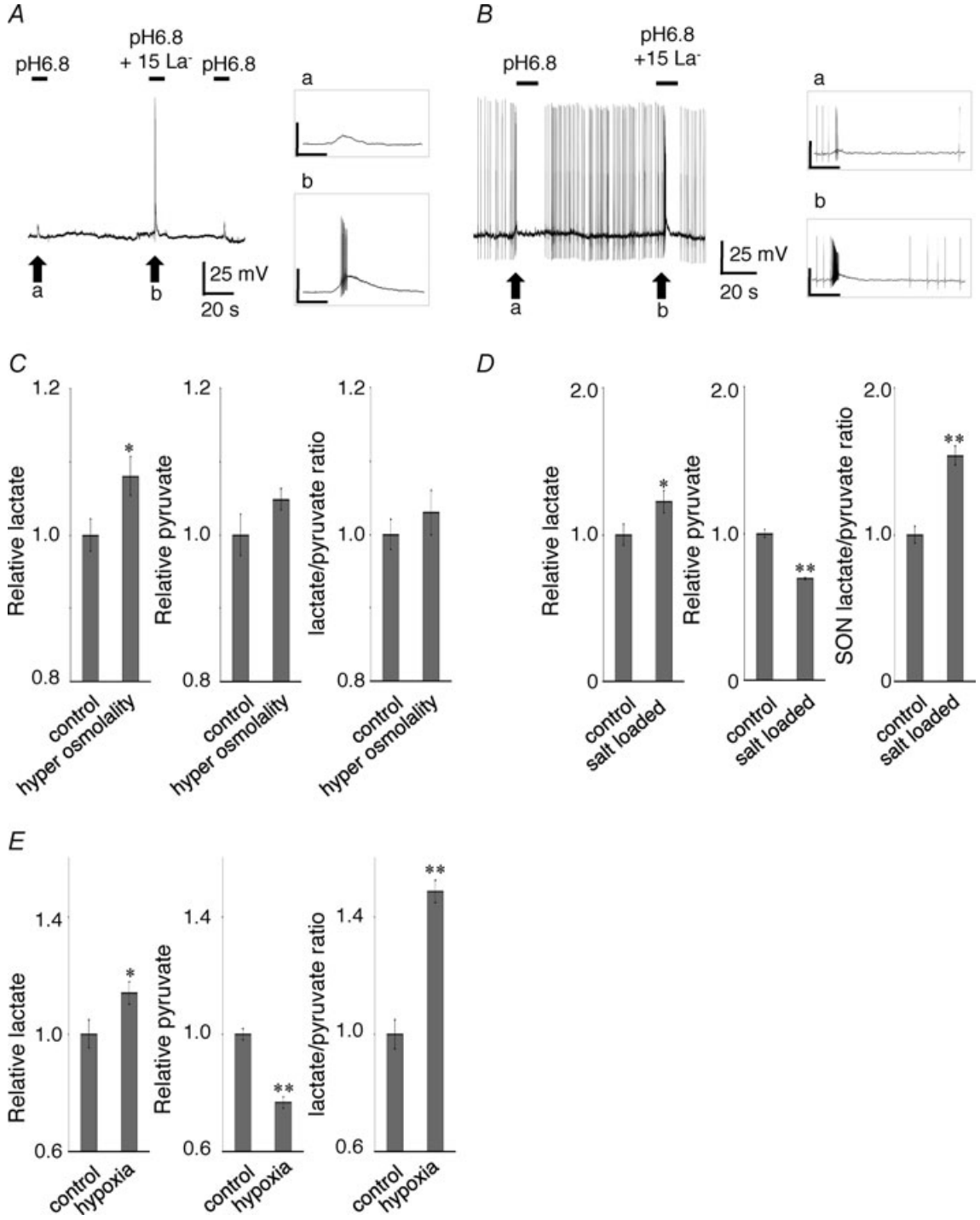

Figure 6. Interaction between ASICs and lactate due to hypoxia and hyperosmolarity in the SON
A, typical changes in membrane potential elicited by decreasing pH from 7.4 to 6.8 in the presence or absence of lactate. Activation of ASIC current by pH 6.8 transiently depolarized the neurons. When pH 6.8 external solution with 15 mM lactate was applied, the neuron was depolarized with a train of action potentials at the initial transient depolarization. *B*, when cells were held at a level just around the firing threshold with a current injection, pH 6.8 induced depolarization and action potentials followed by a refractory period. Inset: lactate increased the depolarization and firing number induced by pH 6.8. The scale bar is 50 mV/1 s. *C*, hypertonicity stimulated production of La^- in the SON tissue but not production of pyruvate. *D*, the tissue La^- level in the SON was significantly increased after osmotic stimulation resulting from salt loading by drinking 2% NaCl for 5 days whereas the tissue pyruvate level was markedly decreased after osmotic stimulation. The tissue La^-:pyruvate ratio was also increased in the SON of salt-loaded rats. *E*, the SON segment incubated under hypoxic conditions

and COS cells (Bassilana *et al.* 1997; Baron *et al.* 2001, 2008). Furthermore, immunohistochemistry and RT-PCR experiments revealed that these neurons express ASIC1a and ASIC2a, but not the 1b, 2b, 3, and 4 subunits. Although these data indicate that the major ASIC-like current of AVP neurons is the heteromeric ASIC1a+ASIC2a current, certain issues remain unresolved. First, we cannot completely exclude involvement of ASIC2b. ASIC2b is known to induce a sustained outward-rectifying non-selective cationic current when associated with other ASIC subunits. Since we occasionally recorded a sustained plateau phase following the peak current in our study, participation of ASIC2b cannot be ruled out. Second, we could not definitively identify the ASIC1a+ASIC2a heteromer in AVP neurons. Although PcTX1 is considered a highly potent inhibitor of ASIC1 that has no effect on wild type ASIC1/ASIC2 heteromers, there are reports of an interaction with ASIC1/*mut*ASIC2 heteromers (Salinas *et al.* 2006; Qadri *et al.* 2009). In addition, there are multiple reports of PcTX1 potentiating or activating ASIC1 in various situations (Chen *et al.* 2005, 2006). In the present study, the ASIC-like currents in AVP neurons were not modulated by PcTX1 at concentrations of 100 nM or 1 μM, which is probably high enough to produce a maximal effect (Salinas *et al.* 2006; Qadri *et al.* 2009). Further biochemical evidence is needed to confirm the molecular composition of the channels. Despite these limitations, our results strongly suggest that the ASIC1a+ASIC2a heteromer is the predominant ASIC subtype expressed in the majority of SON AVP neurons. We further showed that activation of ASIC-like currents increases membrane depolarization dependent on extracellular pH, indicating that acid-induced currents mediated by functional ASICs increase the excitability of AVP neurons.

La^- potentiates the acid-induced excitability of AVP-eGFP neurons

A recent study showed that angiogenesis induced by osmotic stimulation is related to tissue hypoxia in the rat hypothalamus (Alonso *et al.* 2008). An osmotic stimulus increases the release of endogenous AVP from dendrites and cell bodies located in the hypothalamic magnocellular nucleus into the intercellular space within the nucleus. It is probable that dendritic release of AVP, which is generally considered a potent vasoconstrictor, could reduce the oxygen supply to SON via vasoconstrictive effects on the contractile arterioles afferent to the SON resulting in local tissue hypoxia (Alonso *et al.* 2008). Hypoxia is one of the interacting factors that cause an increase in La^- production and concentration in the brain (Vannucci & Hagberg, 2004). Furthermore, the role of extracellular La^- in enhancing the activity of ASICs through chelation of extracellular calcium is known to involve modulation of ASIC1a and ASIC3 (Immke & McCleskey, 2001). Based on these reports and the present results, we hypothesize that La^- generated during local hypoxia induced by osmotic stimulation modifies the function of rat AVP neurons through enhancement of ASIC 1a and 2a. Our electrophysiological data showed that the proton-induced current was potentiated in the presence of extracellular La^- in a concentration-dependent manner. Calcium ions block the ASICs as a result of competition between Ca^{2+} and H^+ at the activation site (Immke & McCleskey, 2003; Paukert *et al.* 2004), and lactate binds and diminishes extracellular free Ca^{2+}, thereby allowing the channel to open at lower H^+ concentrations (Immke & McCleskey, 2003). In the present study, the effects of lactate on acid-induced current increased with pH (Fig. 4*B*), consistent with Ca^{2+}/H^+ competition. The observation that La^- had an effect only when applied with the acidic solutions indicates that La^- does not use a separate receptor and signalling cascade in AVP neurons, consistent with a previous report (Immke & McCleskey, 2001). The ASIC current enhancement induced by lactate was Ca^{2+} concentration dependent and was eliminated under low extracellular Ca^{2+} conditions, indicating that the effects of lactate are due to calcium chelation in the AVP neurons, also in agreement with previous reports (Immke & McCleskey, 2001, 2003). Other monocarboxylic acids (particularly pyruvate and formate) mimicked the effect of La^- in these neurons, further supporting this mechanism. We also showed that La^- increased membrane depolarization and firing number in acid-induced action potentials, suggesting that La^- may play a critical role in regulating neuronal activity.

In contrast, hyperosmolality had no direct effect on the acid-induced current amplitude, lactate enhancement, or desensitization, indicating that there is negligible hyperosmolality sensitivity with respect to peak current or desensitization, which appears to involve a proton-requiring conformation change (Askwith *et al.* 2001; Immke & McCleskey, 2003).

Pathological significance

To address the hypothesis described above, we measured La^- and pyruvate concentrations in the SON from euhydrated or salt-loaded rats. As expected, a significant

with 85% N_2–10% O_2–5% CO_2 showed higher La^- secretion and lower pyruvate secretion than the segment in normoxic conditions with 95% air–5% CO_2. The La^-:pyruvate ratio in the medium released from SON was significantly increased under hypoxia.

increase in the tissue La^- level and La^-:pyruvate ratio was observed in salt-loaded but not euhydrated rats, indicating that La^- production and release in the SON was stimulated under osmotic stress *in vivo*. Hypoxic conditions *in vitro* mimicked this shift in the La^-:pyruvate ratio, further supporting our hypothesis. The ratio of La^- to pyruvate is viewed as an indicator of cytosolic NADH/NAD^+ redox potential due to an equilibration established by the lactate dehydrogenase reaction, $La^- + NAD \rightleftharpoons$ pyruvate + NADH (Barron *et al.* 1997). Hypoxia increases La^- and decreases pyruvate as a result of an increase in NADH redox that is induced, at least in part, by inhibiting mitochondrial respiration in vascular endothelial cells (Barron *et al.* 1997; Gao & Wolin, 2008). These metabolic responses occur not only in endothelial cells but also in neurons and glial cells (Gladden, 2004). Our findings in SON segments containing these cells provide a plausible explanation for the increase in NADH redox and induction of opposite shifts in the La^- and pyruvate concentrations in SON during local hypoxia *in vivo*.

We also measured release of La^- and pyruvate from SON tissue into the incubation medium under normal and hypertonic conditions. La^- release from the SON increased under hypertonic, but not isotonic, conditions, whereas there was no change in pyruvate production. In isolated brain tissues, neurons do not rely on blood supply for oxygen. It is therefore unlikely that local hypoxia underlies this hypertonicity-induced lactate release *in vitro*, and our findings may imply the existence of another mechanism. As suggested previously (Gladden, 2004), it is possible that the action potentials of neuronal activity result in Na^+ entry and K^+ efflux, which in turn activate Na^+,K^+-ATPase leading to production of La^-.

Although La^- can be considered a central player in cellular and whole body metabolism (Gladden, 2004), the resting concentration of La^- in the extracellular fluid of the brain remains controversial with previous estimates predicting a concentration of approximately 1 mM (Silver & Erecińska, 1994; Ronne-Engström *et al.* 1995; Chih *et al.* 2001). The extracellular concentration of lactate in the brain appears to be variable and dependent on various factors such as the area being measured. Although La^- is generated in the CNS during tissue hypoxia/anoxia (Vannucci *et al.* 1994; Ronne-Engström *et al.* 1995; Shimizu *et al.* 2007), the extent by which the extracellular lactate concentration rises in the local SON during osmotic stress remains unknown. Future experiments will provide more precise measurements of the extracellular lactate concentration in local SON.

Taken together, our findings indicate that La^- is produced by SON cells during local hypoxia induced by osmotic stress, leading to a reduction in extracellular Ca^{2+} concentration that in turn increases the sensitivity of ASICs to protons in AVP neurons. These interactions play important roles in the regulatory mechanism of body fluid homeostasis.

References

Akopian AN, Chen CC, Ding Y, Cesare P & Wood JN (2000). A new member of the acid-sensing ion channel family. *Neuroreport* **11**, 2217–2222.

Alonso G, Gallibert E, Lafont C & Guillon G (2008). Intrahypothalamic angiogenesis induced by osmotic stimuli correlates with local hypoxia: a potential role of confined vasoconstriction induced by dendritic secretion of vasopressin. *Endocrinology* **149**, 4279–4288.

Alvarez de la Rosa D, Zhang P, Shao D, White F & Canessa CM (2002). Functional implications of the localization and activity of acid-sensitive channels in rat peripheral nervous system. *Proc Natl Acad Sci U S A* **99**, 2326–2331.

Askwith CC, Benson CJ, Welsh MJ & Snyder PM (2001). DEG/ENaC ion channels involved in sensory transduction are modulated by cold temperature. *Proc Natl Acad Sci U S A* **98**, 6459–6463.

Baron A, Schaefer L, Lingueglia E, Champigny G & Lazdunski M (2001). Zn^{2+} and H^+ are coactivators of acid sensing ion channels. *J Biol Chem* **276**, 35361–35367.

Baron A, Voilley N, Lazdunski M & Lingueglia E (2008). Acid sensing ion channels in dorsal spinal cord neurons. *J Neurosci* **28**, 1498–1508.

Barron JT, Gu L & Parrillo JE (1997). Cytoplasmic redox potential affects energetics and contractile reactivity of vascular smooth muscle. *J Mol Cell Cardiol* **29**, 2225–2232.

Bassilana F, Champigny G, Waldmann R, de Weille JR, Heurteaux C & Lazdunski M (1997). The acid-sensitive ionic channel subunit ASIC and the mammalian degenerin MDEG form a heteromultimeric H^+-gated Na^+ channel with novel properties. *J Biol Chem* **272**, 28819–28822.

Brockway LM, Benos DJ, Keyser KT & Kraft TW (2005). Blockade of amiloride-sensitive sodium channels alters multiple components of the mammalian electroretinogram. *Vis Neurosci* **22**, 143–151.

Bubien JK, Ji H-L, Gillespie GY, Fuller CM, Markert JM, Mapstone TB & Benos DJ (2004). Cation selectivity and inhibition of malignant glioma Na^+ channels by Psalmotoxin 1. *Am J Physiol Cell Physiol* **287**, C1282–C1291.

Chen CC, England S, Akopian AN & Wood JN (1998). A sensory neuron-specific, proton-gated ion channel. *Proc Natl Acad Sci U S A* **95**, 10240–10245.

Chen X, Kalbacher H & Gründer S (2005). The tarantula toxin psalmotoxin 1 inhibits acid-sensing ion channel (ASIC) 1a by increasing its apparent H^+ affinity. *J Gen Physiol* **126**, 71–79.

Chen X, Kalbacher H & Gründer S (2006). Interaction of acid-sensing ion channel (ASIC) 1 with the tarantula toxin psalmotoxin 1 is state dependent. *J Gen Physiol* **127**, 267–276.

Chih CP, Lipton P & Robert ER Jr (2001). Do active cerebral neurons really use lactate rather than glucose? *Trends Neurosci* **24**, 573–478.

Donier E, Rugiero F, Okuse K & Wood JN (2005). Annexin II light chain p11 promotes functional expression of acid-sensing ion channel ASIC1a. *J Biol Chem* **280**, 38666–38672.

Drummond GB (2009). Reporting ethical matters in *The Journal of Physiology*: standards and advice. *J Physiol* **587**, 713–719.

Duan B, Wu LJ, Yu YQ, Ding Y, Jing L, Xu L, Chen J & Xu TL (2007). Upregulation of acid-sensing ion channel ASIC1a in spinal dorsal horn neurons contributes to inflammatory pain hypersensitivity. *J Neurosci* **27**, 11139–11148.

Escoubas P, Bernard C, Lambeau G, Lazdunski M & Darbon H (2003). Recombinant production and solution structure of PcTx1, the specific peptide inhibitor of ASIC1a proton-gated cation channels. *Protein Sci* **12**, 1332–1343.

Escoubas P, De Weille JR, Lecoq A, Diochot S, Waldmann R, Champigny G, Moinier D, Menez A & Lazdunski M (2000). Isolation of a tarantula toxin specific for a class of proton-gated Na^+ channels. *J Biol Chem* **275**, 25116–25121.

Foulkes T, Nassar MA, Lane T, Matthews EA, Baker MD, Gerke V, Okuse K, Dickenson AH & Wood JN (2006). Deletion of annexin 2 light chain p11 in nociceptors causes deficits in somatosensory coding and pain behaviour. *J Neurosci* **26**, 10499–10507.

Gao J, Duan B, Wang DG, Deng XH, Zhang GY, Xu L & Xu TL (2005). Coupling between NMDA receptor and acid-sensing ion channel contributes to ischemic neuronal death. *Neuron* **48**, 635–646.

Gao Q & Wolin MS (2008). Effects of hypoxia on relationships between cytosolic and mitochondrial NAD(P)H redox and superoxide generation in coronary arterial smooth muscle. *Am J Physiol Heart Circ Physiol* **295**, H978–H989.

Garcia-Anoveros J, Derfler B, Neville-Golden J, Hyman BT & Corey DP (1997). BNaC1 and BNaC2 constitute a new family of human neuronal sodium channels related to degenerins and epithelial sodium channels. *Proc Natl Acad Sci U S A* **94**, 1459–1464.

Gladden LB (2004). Lactate metabolism: a new paradigm for the third millennium. *J Physiol* **558**, 5–30.

Grunder S, Geissler HS, Bassler EL & Ruppersberg JP (2000). A new member of acid-sensing ion channels from pituitary gland. *Neuroreport* **11**, 1607–1611.

Hirasawa M, Mouginot D, Kozoriz MG, Kombian SB & Pittman QJ (2003). Vasopressin differentially modulates non-NMDA receptors in vasopressin and oxytocin neurons in the supraoptic nucleus. *J Neurosci* **23**, 4270–4277.

Immke DC & McCleskey EW (2001). Lactate enhances the acid-sensing Na^+ channel on ischemia-sensing neurons. *Nat Neurosci* **4**, 869–870.

Immke DC & McCleskey EW (2003). Protons open acid-sensing ion channels by catalyzing relief of Ca^{2+} blockade. *Neuron* **37**, 75–84.

Jasti J, Furukawa H, Gonzales EB & Gouaux E (2007). Structure of acid-sensing ion channel 1 at 1.9 A resolution and low pH. *Nature* **449**, 316–323.

Kabashima N, Shibuya I, Ibrahim N, Ueta Y & Yamashita H (1997). Inhibition of spontaneous EPSCs and IPSCs by presynaptic $GABA_B$ receptors on rat supraoptic magnocellular neurons. *J Physiol* **504**, 113–126.

Kawamata T, Ninomiya T, Toriyabe M, Yamamoto J, Niiyama Y, Omote K & Namiki A (2006). Immunohistochemical analysis of acid-sensing ion channel 2 expression in rat dorsal root ganglion and effects of axotomy. *Neuroscience* **143**, 175–187.

Kellenberger S & Schild L (2002). Epithelial sodium channel/degenerin family of ion channels: a variety of functions for a shared structure. *Physiol Rev* **82**, 735–767.

Krishtal O (2003). The ASICs: signalling molecules? Modulators? *Trends Neurosci* **26**, 477–483.

Leng G, Brown CH & Russell JA (1999). Physiological pathways regulating the activity of magnocellular neurosecretory cells. *Prog Neurobiol* **57**, 625–655.

Li C, Tripathi PK & Armstrong WE (2007). Differences in spike train variability in rat vasopressin and oxytocin neurons and their relationship to synaptic activity. *J Physiol* **581**, 221–240.

Lingueglia E (2007). Acid-sensing ion channels in sensory perception. *J Biol Chem* **282**, 17325–17329.

Lingueglia E, de Weille JR, Bassilana F, Heurteaux C, Sakai H, Waldmann R & Lazdunski M (1997). A modulatory subunit of acid sensing ion channels in brain and dorsal root ganglion cells. *J Biol Chem* **272**, 29778–29783.

Meltzer RH, Kapoor N, Qadri YJ, Anderson SJ, Fuller CM & Benos DJ (2007). Heteromeric assembly of acid-sensitive ion channel and epithelial sodium channel subunits. *J Biol Chem* **282**, 25548–25559.

Miesenbock G, De Angelis DA & Rothman JE (1998). Visualizing secretion and synaptic transmission with pH-sensitive green fluorescent proteins. *Nature* **394**, 192–195.

Nagae M, Hiraga T & Yoneda T (2007). Acidic microenvironment created by osteoclasts causes bone pain associated with tumor colonization. *J Bone Miner Metab* **25**, 99–104.

Ohbuchi T, Yokoyama T, Saito T, Hashimoto H, Suzuki H, Otsubo H, Fujihara H, Suzuki H & Ueta Y (2009). Brain-derived neurotrophic factor inhibits spontaneous inhibitory postsynaptic currents in the rat supraoptic nucleus. *Brain Res* **1258**, 34–42.

Paukert M, Babini E, Pusch M & Gründer S (2004). Identification of the Ca^{2+} blocking site of acid-sensing ion channel (ASIC) 1: implications for channel gating. *J Gen Physiol* **124**, 383–394.

Price MP, Snyder PM & Welsh MJ (1996). Cloning and expression of a novel human brain Na^+ channel. *J Biol Chem* **271**, 7879–7882.

Qadri YJ, Berdiev BK, Song Y, Lippton HL, Fuller CM & Benos DJ (2009). Psalmotoxin-1 docking to human acid-sensing ion channel-1. *J Biol Chem* **284**, 17625–17633.

Ronne-Engström E, Carlson H, Liu Y, Ungerstedt U & Hillered L (1995). Influence of perfusate glucose concentration on dialysate lactate, pyruvate, aspartate, and glutamate levels under basal and hypoxic conditions: a microdialysis study in rat brain. *J Neurochem* **65**, 257–262.

Salinas M, Rash LD, Baron A, Lambeau G, Escoubas P & Lazdunski M (2006). The receptor site of the spider toxin PcTx1 on the proton-gated cation channel ASIC1a. *J Physiol* **570**, 339–354.

Sharif Naeini R, Witty MF, Seguela P & Bourque CW (2006). An N-terminal variant of Trpv1 channel is required for osmosensory transduction. *Nat Neurosci* **9**, 93–98.

Shimizu H, Watanabe E, Hiyama TY, Nagakura A, Fujikawa A, Okado H, Yanagawa Y, Obata K & Noda M (2007). Glial Na_X channels control lactate signaling to neurons for brain $[Na^+]$ sensing. *Neuron* **54**, 59–72.

Silver IA & Erecińska M (1994). Extracellular glucose concentration in mammalian brain: continuous monitoring of changes during increased neuronal activity and upon limitation in oxygen supply in normo-, hypo-, and hyperglycemic animals. *J Neurosci* **14**, 5068–5076.

Smith DW, Buller KM & Day TA (1995). Role of ventrolateral medulla catecholamine cells in hypothalamic neuroendocrine cell responses to systemic hypoxia. *J Neurosci* **15**, 7979–7888.

Suzuki H, Kawasaki M, Ohnishi H, Otsubo H, Ohbuchi T, Katoh A, Hashimoto H, Yokoyama T, Fujihara H, Dayanithi G, Murphy D, Nakamura T & Ueta Y (2009). Exaggerated response of a vasopressin-enhanced green fluorescent protein transgene to nociceptive stimulation in the rat. *J Neurosci* **29**, 13182–13189.

Ueta Y, Fujihara H, Serino R, Dayanithi G, Ozawa H, Matsuda K, Kawata M, Yamada J, Ueno S, Fukuda A & Murphy D (2005). Transgenic expression of enhanced green fluorescent protein enables direct visualization for physiological studies of vasopressin neurons and isolated nerve terminals of the rat. *Endocrinology* **146**, 406–413.

Vannucci RC, Yager JY & Vannucci SJ (1994). Cerebral glucose and energy utilization during the evolution of hypoxic-ischemic brain damage in the immature rat. *J Cereb Blood Flow Metab* **14**, 279–288.

Vannucci SJ & Hagberg H (2004). Hypoxia-ischemia in the immature brain. *J Exp Biol* **207**, 3149–3154.

Vila-Carriles WH, Kovacs GG, Jovov B, Zhou Z-H, Pahwa AK, Colby G, Esimai O, Gillespie GY, Mapstone TB, Markert JM, Fuller CM, Bubien JK & Benos DJ (2006). Surface expression of ASIC2 inhibits the amiloride-sensitive current and migration of glioma cells. *J Biol Chem* **281**, 19220–19232.

Voilley N (2004). Acid-sensing ion channels (ASICs): new targets for the analgesic effects of non-steroid anti inflammatory drugs (NSAIDs). *Curr Drug Targets Inflamm Allergy* **3**, 71–79.

Voilley N, de Weille J, Mamet J & Lazdunski M (2001). Nonsteroid anti-inflammatory drugs inhibit both the activity and the inflammation-induced expression of acid-sensing ion channels in nociceptors. *J Neurosci* **21**, 8026–8033.

Vukicevic M, Weder G, Boillat A, Boesch A & Kellenberger S (2006). Trypsin cleaves acid-sensing ion channel 1a in a domain that is critical for channel gating. *J Biol Chem* **281**, 714–722.

Waldmann R, Champigny G, Bassilana F, Heurteaux C & Lazdunski M (1997). A proton-gated cation channel involved in acid-sensing. *Nature* **386**, 173–177.

Waldmann R, Champigny G, Voilley N, Lauritzen I & Lazdunski M (1996). The mammalian degenerin MDEG, an amiloride-sensitive cation channel activated by mutations causing neurodegeneration in *Caenorhabditis elegans*. *J Biol Chem* **271**, 10433–10436.

Wemmie JA, Chen J, Askwith CC, Hruska-Hageman AM, Price MP, Nolan BC, Yoder PG, Lamani E, Hoshi T, Freeman JH Jr & Welsh MJ (2002). The acid-activated ion channel ASIC contributes to synaptic plasticity, learning, and memory. *Neuron* **34**, 463–477.

Wemmie JA, Price MP & Welsh MJ (2006). Acid-sensing ion channels: advances, questions and therapeutic opportunities. *Trends Neurosci* **29**, 578–586.

Xiong ZG, Zhu XM, Chu XP, Minami M, Hey J, Wei WL, MacDonald JF, Wemmie JA, Price MP, Welsh MJ & Simon RP (2004). Neuroprotection in ischemia: blocking calcium-permeable acid-sensing ion channels. *Cell* **118**, 687–698.

Xu TL, Li JS & Akaike N (1999). Functional properties of ionotropic glutamate receptor channels in rat sacral dorsal commissural neurons. *Neuropharmacology* **38**, 659–670.

Ye J-H, Gao J, Wu Y-N, Hu Y-J, Zhang C-P & Xu T-L (2007). Identification of acid-sensing ion channels in adenoid cystic carcinomas. *Biochem Biophys Res Commun* **355**, 986–992.

Author contributions

Y.U. designed the research; T.O. and K.S. performed the research; Y.U. coordinated the study, participated in data collection and wrote the paper together with H.S., Y.O., G.D. and D.M. All authors discussed the results, commented on the manuscript and approved the version to be published.

Acknowledgements

We thank Dr Charles W. Bourque (Centre for Research in Neuroscience, McGill University, Canada) for very helpful discussions. This study was supported by Grant-in-Aid for Scientific Research on Priority Areas, No 18077006 to Y.U. from the Ministry of Education, Culture, Sports, Science, and Technology, Japan.